PAPER • OPEN ACCESS

CFD Studies on Triangular Micro-Vortex Generators in Flow Control

To cite this article: V Yashodhar *et al* 2017 *IOP Conf. Ser.: Mater. Sci. Eng.* **184** 012007

View the article online for updates and enhancements.

CFD Studies on Triangular Micro-Vortex Generators in Flow Control

Yashodhar V[1], Humrutha G[2], M Kaushik[3], and S A Khan*[4]

[1,2,3]Department of Aerospace Engineering, Indian Institute of Technology Kharagpur-721302, India
[4]Department of Mechanical Engineering, International Islamic university, Kualalumpur, Malaysia

E-mail: [3]mkaushik@aero.iitkgp.ernet.in, [4*]sakhan@iium.edu.my

Abstract. In the present study, the flow characteristics of the commercially used S809 wind turbine airfoil controlled with triangular counter-rotating micro-vortex generators at stall angle of attack of 15 degrees and 10 m/s, 15 m/s and 20 m/s (speed range used in the wind turbine applications) had been computationally investigated. In addition to the controlled airfoil, an uncontrolled airfoil was also studied for the comparison. The modelling and analysis had been carried out using incompressible, Reynolds Averaged Navier Stokes equation using Spalart-Allmaras one equation turbulence model. The numerical computations were performed with SIMPLE algorithm. The velocity profiles at different locations on the suction surface were plotted for both uncontrolled and controlled airfoils. The shear stresses exerted on the upper surface of the airfoil in both the configurations were also compared. It is found that the controlled airfoil, the shear stress distribution was greatly increased near to trailing edge of the airfoil revealing the superiority of vortex generators in increasing the efficiency of wind turbine by delaying boundary layer separation. The qualitative results of flow visualization in the spanwise direction also support the quantitative findings of velocity profiles and shear stress distribution.

Keywords: Micro-vortex generators, Boundary layer separation, Stream-wise vortices, Critical shear stress, Flow visualization

Nomenclature

MVG	=	Micro-vortex generator
h	=	Height of micro-vortex generator
δ	=	Boundary layer thickness
α	=	Vertex angle of triangular micro-vortex generator
β	=	Angle of attack
Z	=	Length between adjacent micro vortex generators
c	=	Chord of the airfoil
x	=	X-axis (measured from the leading edge of the airfoil)
U_∞	=	Free-stream velocity

τ	=	RMS values of surface shear stress
Tc	=	Critical shear stress
RANS	=	Reynolds Averaged Navier Stokes

1. Introduction

In aircrafts, the surface roughness or placement of micro-vortex generators over wing delays boundary layer separation and hence increases lift thereby increasing stall angle. The optimized MVG-controlled flow over airfoil increases its aerodynamic efficiency. The boundary layer separation is the most critical problem for the wind turbines which reduces its performance the necessity of flow control arises. Micro-vortex generators are small trapezoid shaped fin-like devices, which are used in aircrafts to improve their aerodynamic efficiency. Since long they are considered as a cost effective solution due to their ease in manufacturing and installation over wings. They greatly influence the aerodynamic forces and stall characteristics by controlling the flow over the wind turbine rotors as well. Generally wind turbines can be classified into two types, pitch controlled turbines which alter the pitch of the rotor and Stall controlled turbines which stall the entire turbine, if the RPM exceeds a certain value. The MVGs are best suited for the stall controlled wind turbines. Khalfallaha and Koliub (2007) studied the advantages of micro-vortex generators in flow control and dust removal in dusty regions where power losses can aggravate up to 57% in the span of nine months **Error! Reference source not found.**. They performed their experimental study to see the effect of dust accumulation on rotor blades of a stall regulated 300 kW wind turbine for a period of one year. They found that the location of dust deposition is dominated near the stagnation points. They have also concluded that the area of dust deposition and dust particle size increases with lapse of time. These dust particles were found to affect the aerodynamic loads on the rotors which has led to decrease in lift and increase in drag. Further, it was reported that the roughness effects resulting in degradation, depends on the roughness length relative to Boundary layer thickness, Reynolds number and Airfoil type. Nianxin and Jinping (2009) performed a computational study on the flow past a wind turbine blade to investigate the effect of roughness size and roughness area covered on the lift and drag coefficients **Error! Reference source not found.**. It is found that airfoils are more sensitive to surface roughness if they are located in the former 50% chord than the latter half. The lift coefficient experienced a decrease of about 30% in the extreme case at the roughness location of 25% chord. It was also seen that the roughness at the critical locations promote premature turbulence and flow separation. It is known that the vortex generators promote turbulence which leads to losses in the wake region of the airfoil. Hence to minimize these losses, the dimensions of the vortex generators must be precise. Bray (1998) has performed his studies on the efficiency of vortex generators in delaying flow separation and reducing boundary layer thickness. He found that the flow control through manipulation of the boundary layer either in preventing or delaying the separation has significant positive effects on the lift and performance of aircraft **Error! Reference source not found.**In the recent past, many studies have been performed on various geometries of the vortex generators under adverse pressure gradient. Gad-el-Hak (2000) has predicted the point of boundary layer separation using various low profile vortex generators. He concluded that the introduction of high momentum flow into the boundary layer is one of the most efficient methods in delaying the flow separation which eventually enhances the performance **Error! Reference source not found.**. The micro-vortex generators generally fetch turbulence into the wake of the airfoil which eventually leads to losses, therefore its shape and size must be properly designed. Lin (2002) has performed his studies on variable size micro-vortex generators **Error! Reference source not found.**. It was found that the height of the vortex generators must be less than the boundary layer thickness (δ). It was seen that when vortex generator's height (h) was kept 62.5% of the boundary layer thickness then it showed a higher performance than the case when h= δ. Even when the height of MVGs lies in the range of 0.1 < h/δ < 0.2, it provides a sufficient moment transfer into the Boundary layer. Anand et al (2010) have shown in their studies that the optimum MVG geometry and configuration may also depend on the airfoil shape **Error! Reference source not found.**. It is known that the different airfoil shapes has different stall characteristics and they also have different transition

points along the surface. Hence they concluded that a particular MVG configuration optimized for one airfoil profile may not be optimal for another profile of different thickness, camber, or leading-edge radius. The test conducted in low-turbulence pressure wind tunnel at NASA Langley Research Centre (2000) showed that the MVGs dramatically increased the performance of the aircraft **Error! Reference source not found.**. In this study it was also found that the generated noise gets attenuated while landing. It has been shown as one of the cost effective means to improve the performance of an aircraft. Shan et al (2008) have found that the MVGs are advantageous in many aspects as compared to other high lift augmenting devices such as flaps and slats **Error! Reference source not found.**It is seen that for wings or any other lifting surface; the fully attached flow not only leads to increased lift but also minimizes aeroacoustics noise levels. For wind turbine blades these advantages manifest in higher aerodynamic torque and power output for given wind conditions.

From the above, it is evident that most of the studies are concentrated in understanding the flow physics behind the vortex generators applications such as, the formation of separation bubbles, delay of flow separation and boundary layer thinning effects. Although, some investigations have been done on the shape optimization of these vortex generators to improve airfoil performance but the effects on the surface shear stress at high angle of attacks have been hardly looked into. The shear stress distribution is critical for the wind turbine blades. This is because when the blade surface has roughness then it is prone to an early boundary layer separation. From the literature, it is understood that the separation can be delayed by the deployment of the vortex generators over airfoil surface. However, all these vortex generators shape do not improve the wind turbine's performance. Hence, there is a need to optimize MVGs geometry as well as their placement over the wind turbine rotor blade. Keeping view on this objective, an innovative design named as triangular counter rotating micro-vortex generator by combining the vortex manipulation advantages of triangular shape and counter rotating shapes, has been studied as flow control. Thus, the present investigation aims at evaluating and comparing the velocity profiles of the triangular counter rotating micro-vortex generators controlled airfoil with that of plain airfoil configuration. To investigate the MVGs efficacy in delaying boundary layer separation the shear stress was also compared for both uncontrolled and controlled configurations. The commercially used S809 airfoil in wind turbine blades was chosen for the study.

2. Methodology

The micro-vortex generators were used to control the flow over airfoil. In determining the height of vortex generators the thickness of boundary layer at a point about 1 cm upstream of the separation point was calculated. This boundary layer thickness was also used in determining the dimensions of the MVGs. The flow over MVG controlled airfoil configuration had been simulated at the stall angle of attack and the velocity profiles along with shear stress were computed at three different flow speeds. The results obtained were compared with their uncontrolled counterpart under similar flow conditions.

The micro-vortex generators were placed in the mid-span of airfoil just upstream of the separation point. In the present investigation, a counter-rotating configuration and a triangular configuration were merged together in obtaining triangular counter-rotating micro-vortex generators as shown in Figs 2.1(a)-(c).

The three dimensional models were developed using the SOLIDWORKS designing package. These models were imported into the ANSYS design modeler and a flow domain was chosen for the analysis. The control volume was meshed in the ANSYS mesh modeler. The discretization of the domain was done using unstructured grid consisting of approximately 1350000 tetrahedral and hexahedral elements. A fine mesh in the vicinity of the airfoil model was adapted. The cross-sectional views of uncontrolled airfoil mesh and MVG controlled airfoil mesh were shown in the Figs 2.2(a)-(b). It can be seen that the mesh was slightly inflated near the airfoil surface in both uncontrolled and controlled configurations. This was purposefully done to have very fine mesh in the proximity of the suction surface of the airfoil to obtain more accurate flow characteristics. Sufficiently large number of

elements was issued at sharp edges and low curvature points such as near the micro-vortex generators, leading edge and trailing edge of the airfoil.
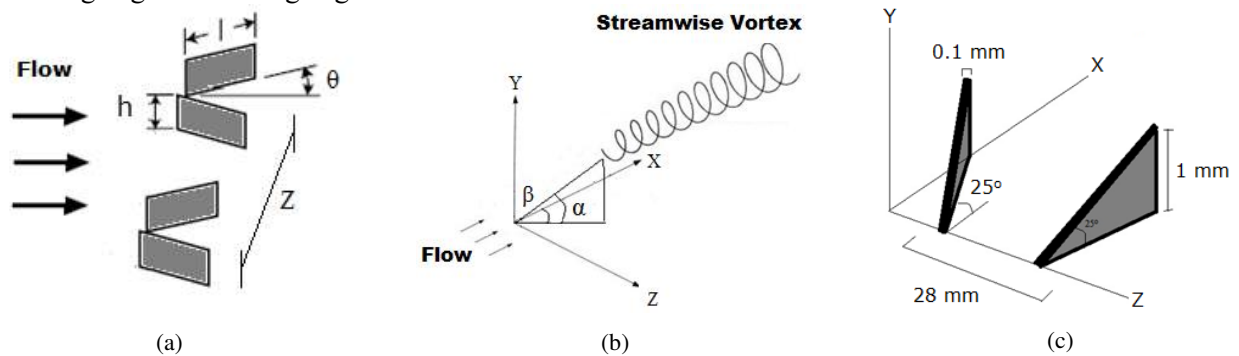

Fig 2.1 Schematic diagrams of micro-vortex generators geometry, (a) Counter-rotating vortex generators, (b) Triangular vortex generators (c) Triangular counter-rotating micro-vortex generators.
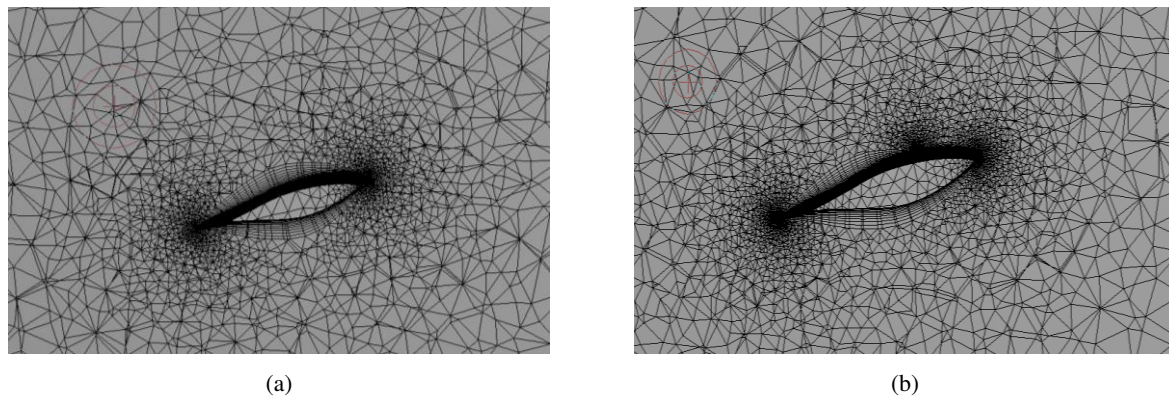

Fig 2.2 Cross-sectional views of the meshed airfoils, (a) uncontrolled airfoil (b) controlled airfoil with MVGs.

The computational flow analysis was done using the FLUENT software package. With air as flowing fluid at incompressible speeds the 3D models were analyzed using RANS equations. The Spalart-Allmaras turbulence model was used to model the Reynolds stresses in the Navier Stokes equations. This turbulence model was a one-equation model that solves a modelled transport equation using the kinematic viscosity. From the literature, it is found that the Spalart-Allmaras model provides accurate results especially when the boundary layer is subjected to an adverse pressure gradient. Also, this model is relatively stable and less sensitive to the grid resolution than the two-equation model **Error! Reference source not found.**. However, the Spalart-Allmaras model suffers from a deficiency common to transport type models that, it fails to predict the reduction in shear layer growth rate with increasing jet Mach number. The model will predict the incompressible shear layer growth rate regardless of the jet Mach number. The SIMPLE scheme was used for pressure-velocity coupling, and pressure and momentum equations are approximated using the second order upwind scheme. Based on chord of the airfoil taken as characteristics length, the Reynolds number were found to be 2×10^5, 3×10^5 and 4×10^5 for the free-stream velocities of 10 m/s, 15 m/s, and 20 m/s, respectively. A no-slip boundary condition was applied on the surface of the airfoil. The inlet turbulence intensity was set to 10% which had closely simulated the atmospheric boundary layer exposure to industrial wind turbine blades.

3. Results and Discussion

From the literature, it is understood that increasing surface roughness delays the boundary layer separation. One such technique to increase the roughness is the deployment of boundary layer submerged vortex generators over the upper surface of airfoil. These MVGs induce shear stress greater than the critical shear

stress required for separation, hence the boundary layer remains attached and thereby increasing the aerodynamic performance of wind turbine blades. Further, since not all the micro-vortex generators shapes improve the aerodynamic performance, thus their design and installation over airfoil surface must be optimized. With this objective, the present computational study was carried out to investigate the efficacy of an innovative design of micro-vortex generators named as, triangular counter rotating micro-vortex generators deployed over the wind turbine S809 airfoil. To quantify the MVGs effects on aerodynamic performance the streamwise velocity profiles were plotted for both uncontrolled and controlled configurations. In addition, the shear stress distributions were also compared to investigate the MVGs effectiveness in delaying boundary layer separation. For qualitative study, the visualization images of velocity magnitude contours were also analyzed.

3.1. Streamwise Velocity Profiles

The streamwise velocity profiles at two different axial locations at free stream velocities of 10 m/s, 15 m/s and 20 m/s are shown in Figs 3.1(a)-(b). The axial locations studied are 0.5c (near field location), and 0.83c (far downstream location). The angle of attack was kept constant at 15 degrees, which is the stall angle for uncontrolled S809 airfoil. The local velocity (u) is plotted against the transverse distance (y) from the surface of the airfoil to obtain the velocity profiles. These plots were not non-dimensionalized purposefully to optimize their presentation.
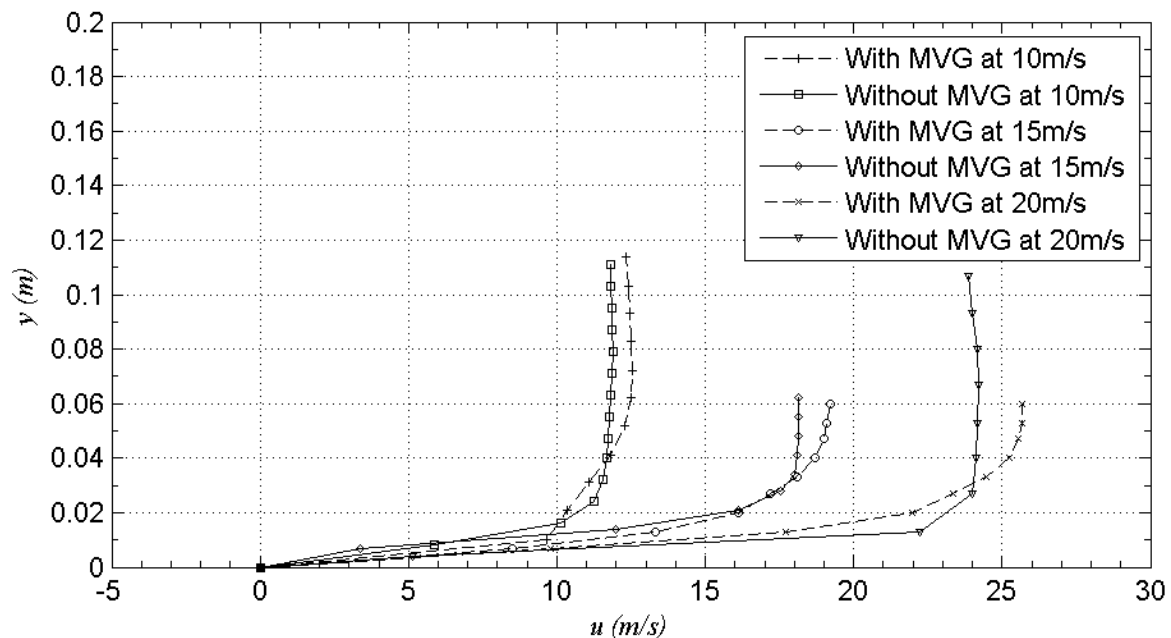

Fig 3.1(a) Streamwise velocity profiles at x/c = 0.5 and β = 15°.

The velocity at x/c = 0.5 and β = 15° for both uncontrolled airfoil and the airfoil controlled with triangular counter rotating micro-vortex generators are shown in Fig 3.1(a). It is seen that the velocity profiles for the controlled airfoil become shallower than the uncontrolled one at all the flow speeds investigated. In other words, there exists a large velocity gradient in transverse direction (y-direction) inside the boundary layer in comparison to the plain airfoil configuration. Since, the height of micro-vortex generators was less than the boundary layer thickness (h/δ = 0.5), thus it induces larger shear stress on the airfoil surface which delays the boundary layer separation thereby increasing aerodynamic performance by minimizing flow separation losses. Thus, the superiority of controlled airfoil configuration over uncontrolled one is established in this case. Further, it is also seen that at the flow speed of 10 m/s both the curves are approaching each other. With the increase of flow speed to 15 m/s, performance of controlled airfoil is slightly inferior to its uncontrolled counterpart. However, when the flow speed is further increased to 20 m/s the controlled airfoil is again exhibiting its superiority in increasing the velocity gradient and hence the shear stress over the airfoil surface. Interestingly, the boundary layer is still attached over the controlled airfoil and thus increasing the stall angle beyond 15°.

When the location is increased to 0.83c (i.e. near to trailing edge of the airfoil), the larger back-flow region at β = 15° is seen in all the uncontrolled cases (Fig 3.1(b)). It is obvious because this zone is highly

vortex dominated. At all the flow speeds the back-flow region is seen and the boundary layer exhibits the tendency of separation at 10 m/s and 15 m/s free stream velocities. That is, there exists a zero-pressure gradient (du/dy =0) at this location for these flow speeds. Interestingly, again at U_∞= 20 m/s the MVG controlled airfoil has maintained its superiority over the uncontrolled airfoil. Hence, at stall angle the boundary layer is completely separated leading to decreased aerodynamic performance. However, the magnitude of the maximum backflow velocity and the width of the back-flow region are greatly reduced in the case of controlled configuration. It again shows the superiority of micro-vortex generators controlled airfoil in improving aerodynamic performance and delaying boundary layer separation than the uncontrolled airfoil.
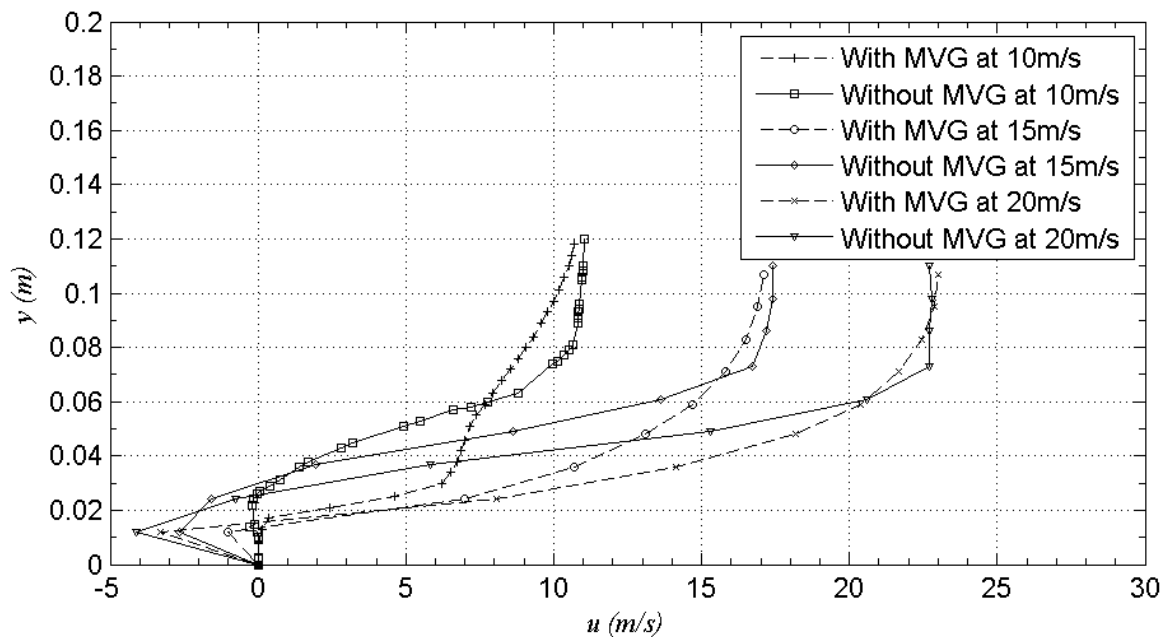

Fig 3.1(b) Streamwise velocity profiles at x/c = 0.83 and β = 15°.

From the above discussions, it is evident that the velocity profiles of the airfoil controlled with the micro-vortex generators have a larger velocity gradient than the plain airfoil. It clearly indicates the formation of shear layers along the surface of the airfoil. Although, the backflow region is reduced in some of the cases but the boundary layer thickness is still greater in case of controlled airfoils. This may be because of the gradual change in velocity due to significant number of shear layers formed.

3.2. Shear Stress Distribution

The shear stress distribution is characterised by the measured root mean square (RMS) stress fluctuations in three dimensions as shown below.

$$\tau = \frac{1}{2}\sqrt{\left(\overline{(\tau_x')^2} + \overline{\left(\tau_y'\right)^2} + \overline{(\tau_z')^2}\right)}$$
(Eq. 1)
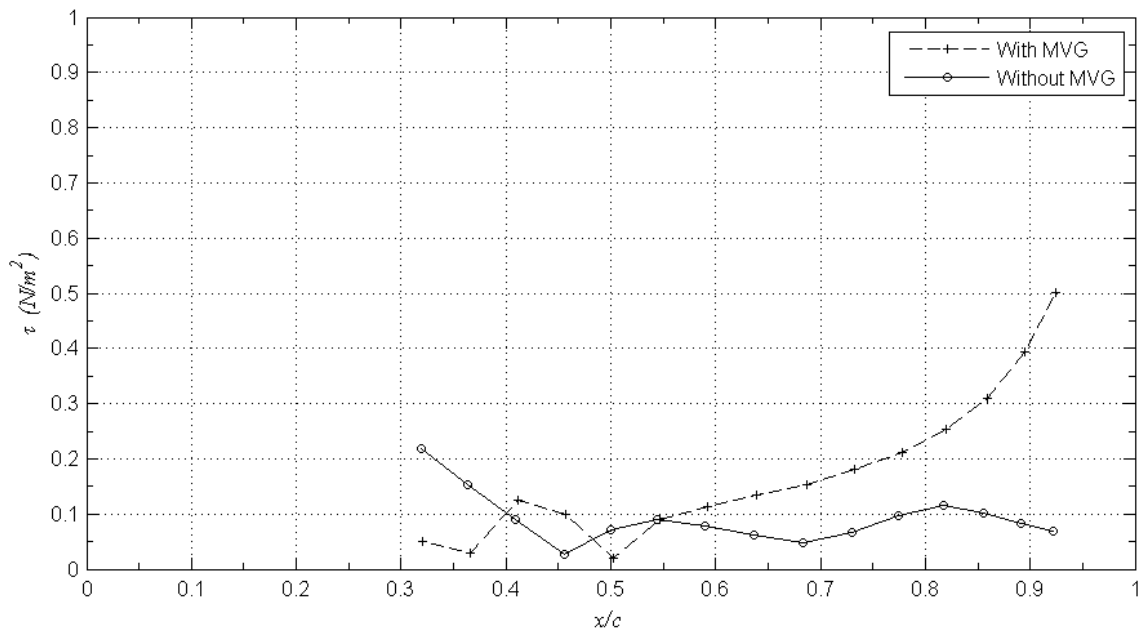
Fig 3.2 Shear stress distribution at $\beta = 15^o$ and $U_\infty = 15$ m/s.

The shear stress distribution at the free-stream velocity of 15 m/s at $\beta = 15^o$ for both uncontrolled airfoil and the airfoil controlled with micro-vortex generators are presented in Fig 3.2.

It was seen that at the stall angle of attack, both uncontrolled and controlled airfoils are possessing almost similar shear stress distribution along the surface. However, in the case of airfoil without controls the shear stress shows a dip at $0.5c$, which could be due to the formation of a small bubble or recirculation zone. In the vicinity of this location the flow is unsteady due to frequent attachment or detachment of the boundary layer and this unsteadiness owe to the acoustic waves which travels upstream are generated through the vortices downstream. Ahead of this location, the curve starts increasing and then decreases again reaching to its minimum at $0.7c$. This may be because of the boundary layer separation taking place at the trailing edge of airfoil. However, when the micro-vortex generators are installed over the suction surface the shear stress is continuously increasing till the trailing edge except at $0.36c$. The increased shear stress on the controlled airfoil surface denotes the larger skin friction. Hence, it has greater ability in delaying the flow separation especially in the far downstream locations.

3.3. *Variation of Pressure Coefficient*

The spanwise average of the coefficient of pressure varying with the chord of the wind turbine airfoil at $\beta = 15^o$ and $U_\infty = 15$ m/s is shown in the Fig 3.3. The pressure coefficient distribution exhibits the considerable increase in negative pressure on the suction side as the boundary layer remains attached due to the deployment of micro-vortex generators. However, a slight increase in the positive pressure on the lower surface is also observed. This distribution suggests the increase in lift on the controlled airfoil compared to the plain one.
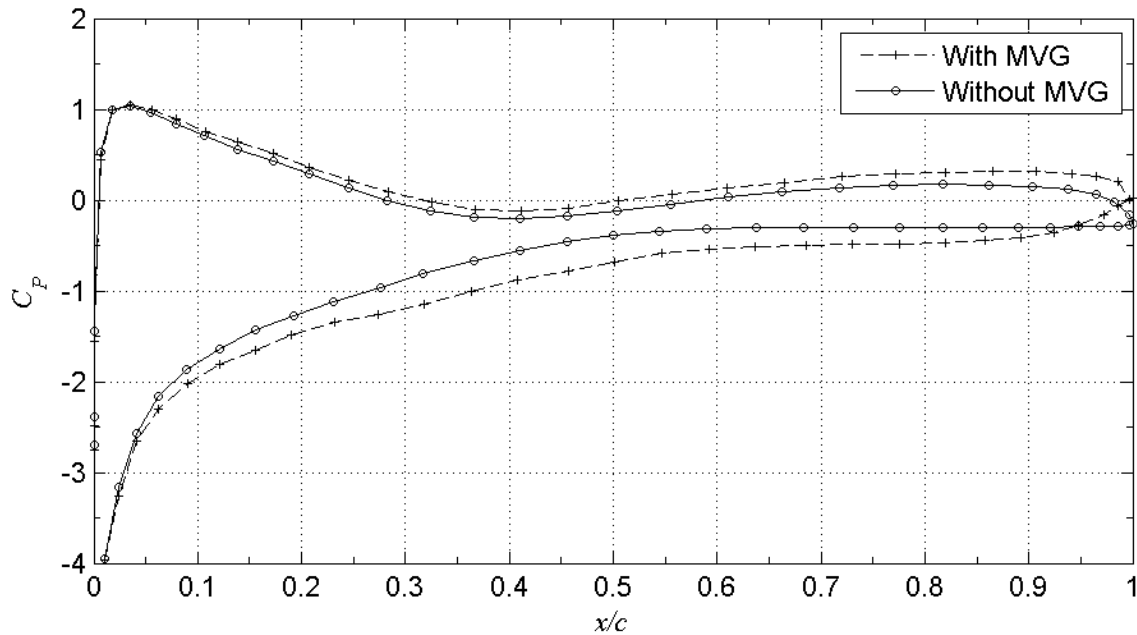
Fig 3.3 C_P distribution for airfoils at and U_∞= 15 m/s.

The experimental results of Somers (1997) are found to be in close agreement with the computed C_P values **Error! Reference source not found.**.

3.4. Flow Field Visualization

In investigating the effectiveness of micro-vortex generators, the flow field was visualized along the spanwise direction for both uncontrolled and controlled airfoil configurations at airfoil stall angle (β = 15°) and free stream velocity of 15 m/s as shown in the Figs 3.4(a)-(b). It can be seen that a large recirculation zone does exist over uncontrolled airfoil near trailing edge due to boundary layer separation at stall angle (Fig 3.4(a)). These trailing edge vortices induce boundary layer separation near to leading edge by sending acoustic information in upstream direction. Therefore, there exists a large recirculation zone near to leading edge.
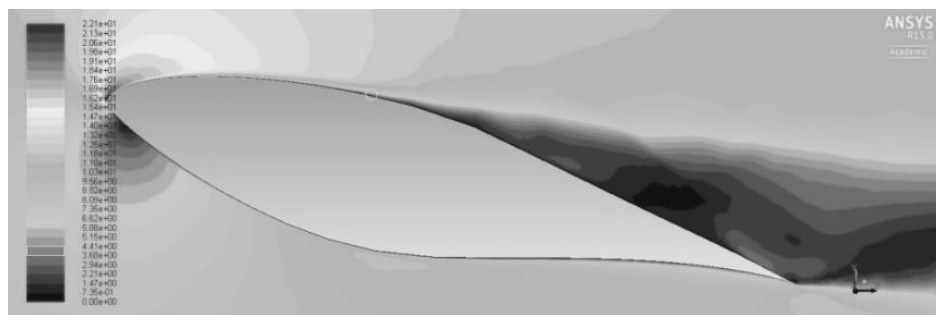
(a)
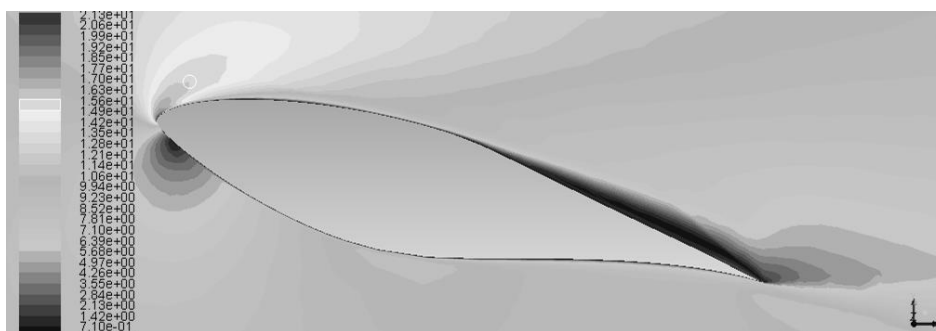
(b)

Fig 3.4 Spanwise flow field visualization of airfoils β = 15° and U_∞= 15 m/s, (a) uncontrolled airfoil, (b) controlled airfoil.

However, once micro-vortex generators were deployed over the suction surface of the airfoil the flow field was seen as given in Fig 3.4(b). It is clearly seen that, the vortices generated by the MVGs delays the boundary layer separation and hence the recirculation zone is suppressed. Hence, due to decreased losses, the performance output of the wind turbine will be increased. These visualization results clearly support the findings obtained in the sections on velocity profiles and shear stress distribution.

4. Conclusions

The quantitative and qualitative results on the efficacy of the proposed triangular counter rotating micro-vortex generators show that the deployment of micro-vortex generator reduces the boundary layer thickness in the flow past them and delays separation. Due to supressed flow recirculation zones on the controlled airfoil surface, the shear stress was found to be linearly increasing. It will lead to further increase in stall angle for controlled configurations beyond the existing 15° stall angle of uncontrolled airfoil. In addition, the images obtained by flow visualization along the spanwise direction show the advantages of micro-vortex generators in improving the aerodynamic performance. Although, the increase in drag may be expected but the drag analysis along with L/D ratio will be performed in the future studies.

References

[1]   Khalfallaha M G and Koliub A M 2007 Effect of dust on the performance of wind turbines *Desalination* **209** 209–220.
[2]   Nianxin R and Jinping Ou 2009 Dust effect on the performance of wind turbine airfoils *J. Electromagnetic Analysis & Applications* **1** 102–107.
[3]   Bray 1998 A parametric studies of vane and air-jet vortex generators (PhD thesis Cranfield University).
[4]   Gad-el-Hak M 2000 Flow control, passive, active, and reactive flow management (Cambridge University Press).
[5]   Lin J C 2002 Review of research on low-profile vortex generators to control boundary-layer separation *Progress in Aerospace Sciences* **38** 389–420.
[6]   Anand et al 2010 Passive flow control over NACA0012 airfoil using vortex generators *Conference on Fluid Mechanics and Fluid Power* (FMFP10 – FP – 12).
[7]   NASA Langley Research Centre 2000 Micro-vortex generators enhance aircraft performance (NASA Fact Sheet FS-2000-06-52-LaRC).
[8]   Shan H et al 2008 Numerical study of passive and active flow separation control over a NACA0012 airfoil *Computers & Fluids* **37** 975–992.
[9]   Yaras M I and Grosvenor A D 2003 Evaluation of one- and two-equation low-Re turbulence models Part II—Vortex-generator jet and diffusing S-duct flows *International Journal for Numerical Methods in Fluids* **42** 1321–1343.
[10]   Somers D 1997 Design and experimental results for the S809 airfoil *National Renewable Energy Laboratory, USA* (NREL/SR-440-6918).